Electronic Supplementary Information (ESI) *for*

Designing All-Inorganic Flexible $Na_{0.5}Bi_{0.5}TiO_3$-Based Film Capacitor with Giant and Stable Energy Storage Performance

Changhong Yang*[ab], Jin Qian[b], Yajie Han[b], Panpan Lv[a], Shifeng Huang,[a] Xin Cheng[a] and Zhenxiang Cheng*[c]

[a.] *Shandong Provincial Key Laboratory of Preparation and Measurement of Building Materials, University of Jinan, Jinan 250022, China.*

[b.] *School of Materials Science and Engineering, University of Jinan, Jinan 250022, China.*

[c.] *Institute for Superconducting and Electronic Materials, Australian Institute for Innovative Materials, University of Wollongong, Innovation Campus, North Wollongong, NSW 2500, Australia.*

*Corresponding Authors:

mse_yangch@ujn.edu.cn (Changhong Yang)

cheng@uow.edu.au (Zhenxiang Cheng)

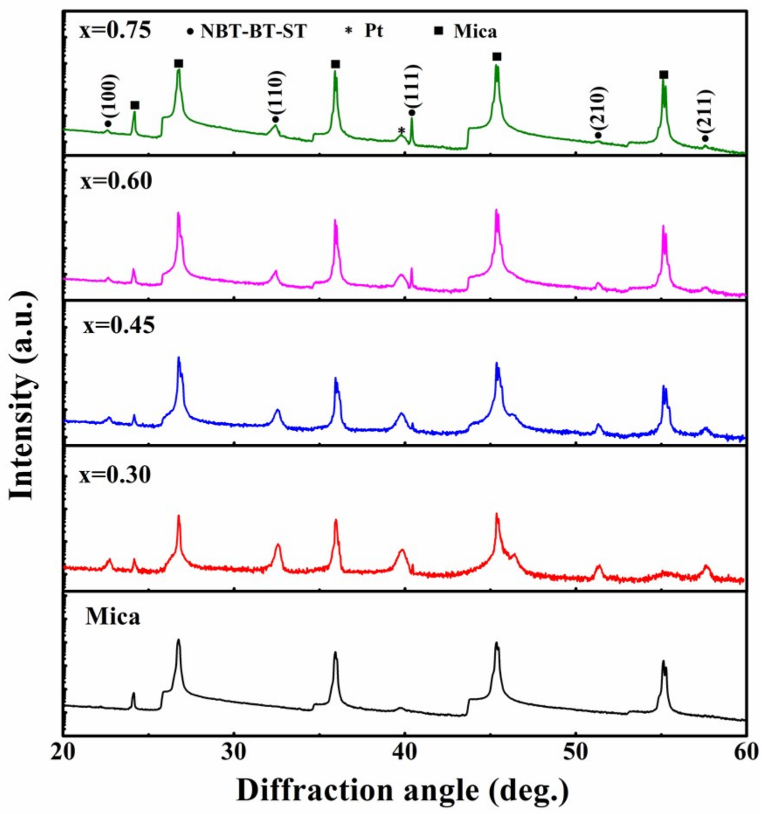

Figure S1. X-ray diffraction patterns of the mica substrate, and Mn:NBT-BT-xST/Pt/mica heterostructures (x=0.30, 0.45, 0.60, 0.75).

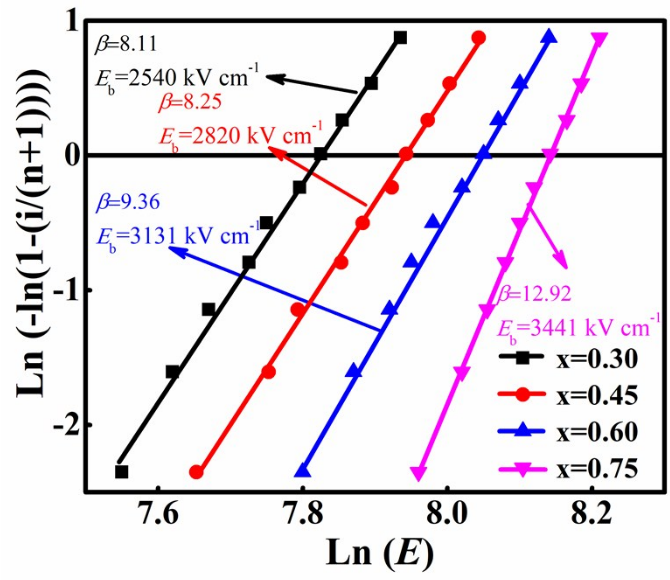

Figure S2. Weibull distributions and the fitting lines for the dielectric breakdown strengths of Mn:NBT-BT-xST (x=0.30, 0.45, 0.60, 0.75) film capacitors.

The characteristic dielectric breakdown strength (E_b) of Mn:NBT-BT-xST thin films were studied by Weibull distribution according to the following equations:

$$X_i = Ln(E_i) \qquad (1)$$

$$Y_i = Ln\left(-\ln\left(1-\frac{i}{n+1}\right)\right) \qquad (2)$$

where E_i is breakdown electric field for each specimen arranged in an ascending order of $E_1 \leq E_2 \leq \ldots E_i \ldots \leq E_n$, i is serial number of specimens, and n is the total number of specimens. Based on the Weibull distribution function, there should be a linear relationship between X_i and Y_i. The average E_b for each film can be extracted from the intersect points of the fitting lines and the horizontal line. As displayed in Figure S2, the slope parameter β, related to the scatter of E_b data, increases from 8.11 at x=0.3 to 12.92 at x=0.75, indicating an enhancement in dielectric reliability by ST incorporation. The E_b are calculated to be 2540, 2820, 3131 and 3441 kV cm^{-1} for the x=0.30, 0.45, 0.60, and 0.75 films, respectively.

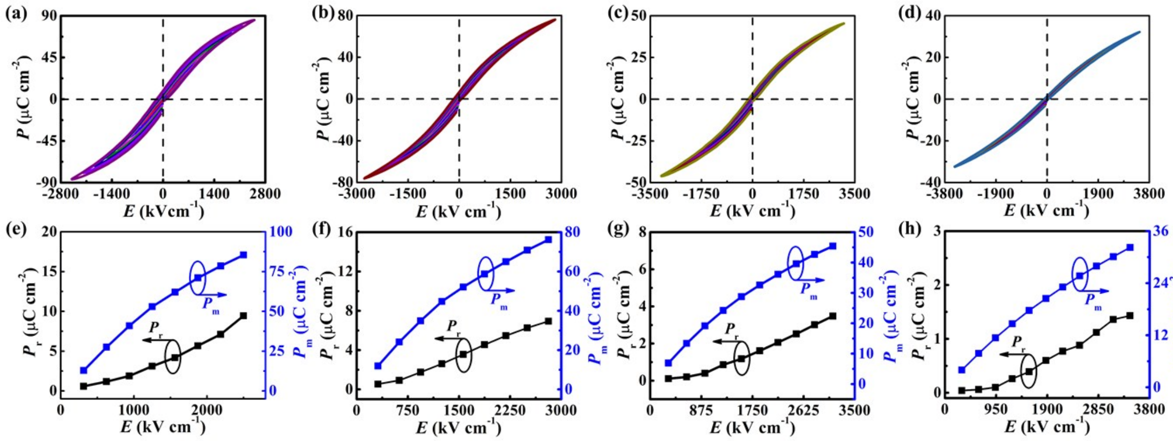

Figure S3. The bipolar *P-E* loops measured from low electric field to E_b, and corresponding P_r and P_m as functions of applied electric field for the Mn:NBT-BT-xST film capacitors: a) & e) x=0.30; b) and f) x=0.45; c) & g) x=0.60; d) & h) x=0.75.

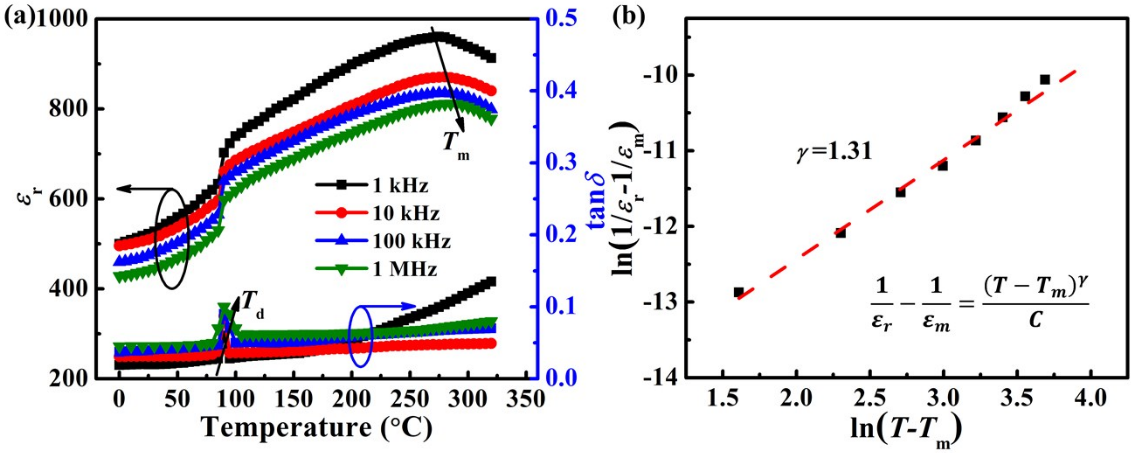

Figure S4. a) The ε_r and tanδ as functions of temperature measured at frequencies from 1 kHz to 1 MHz for the Mn:NBT-BT film capacitor. b) Characterization of γ using the modified Curie-Weiss equation. The depolarization temperature T_d for Mn:NBT-BT film is ~90 °C, and the maximum ε_r occurs at ~280 °C (T_m). Using the modified Curie-Weiss relationship, the diffuseness parameter γ of the Mn:NBT-BT film is estimated to be 1.31, indicating a certain degree of relaxor state in film.

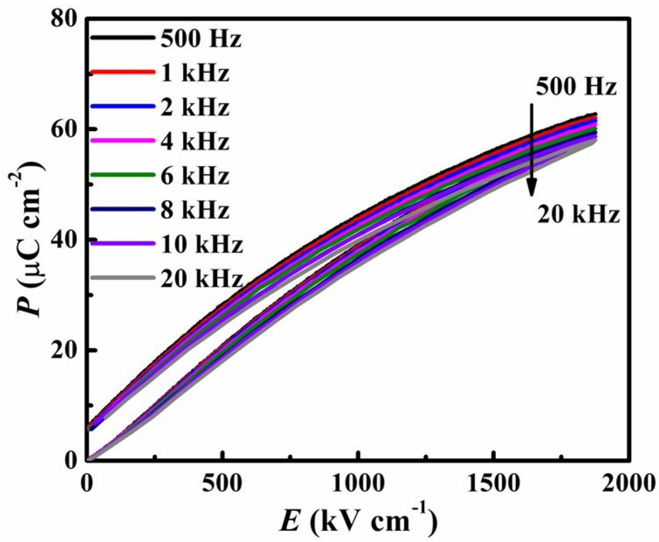

Figure S5. The unipolar *P-E* loops of the Mn:NBT-BT-0.45ST film capacitor measured under 1875 kV cm^{-1} from 500 Hz to 20 kHz at room temperature.

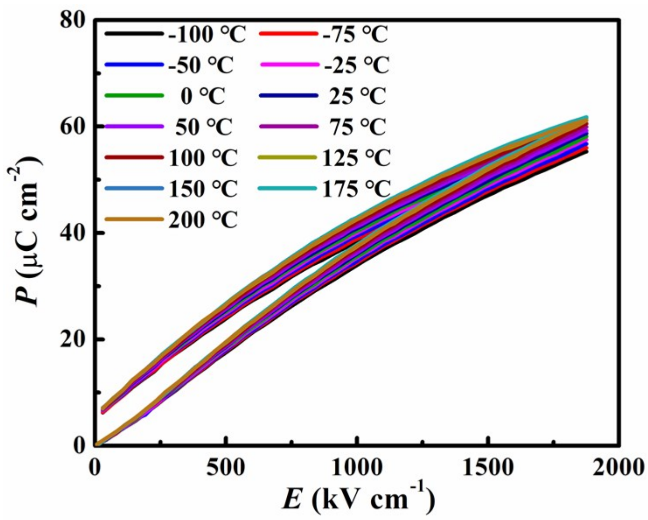

Figure S6. The unipolar *P-E* loops of the Mn:NBT-BT-0.45ST film capacitor measured under 1875 kV cm^{-1} &10 kHz at intervals of 25 °C in the temperature range of -100-200 °C.

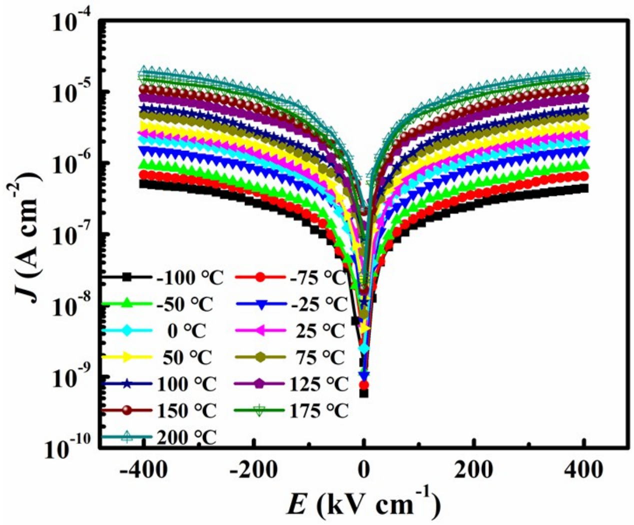

Figure S7. The plots of leakage current density-electric field for the Mn:NBT-BT-0.45ST film capacitor at -100-200 °C.

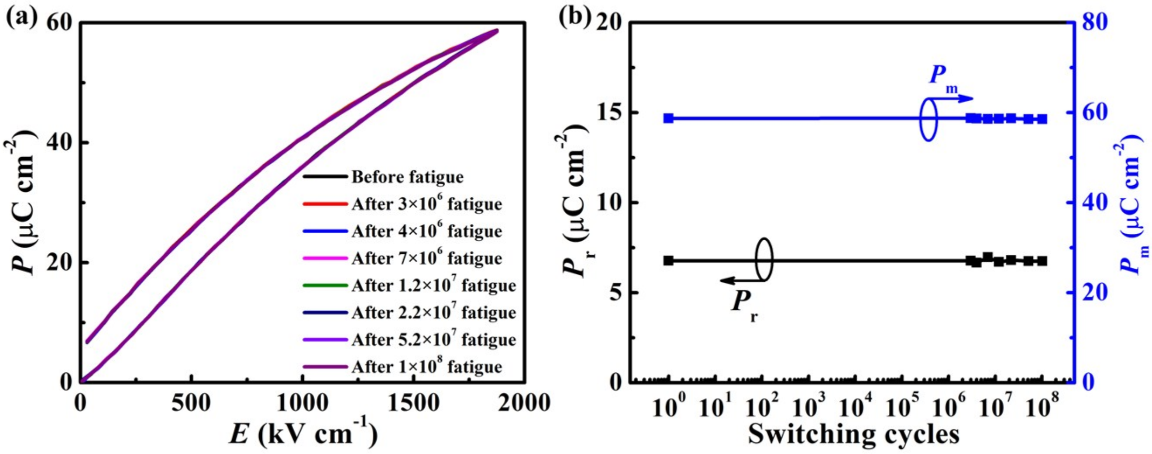

Figure S8. a) The unipolar *P*-*E* loops, and b) corresponding P_r and P_m as functions of switching cycle during the 10^8 charging-discharging cycles of the Mn:NBT-BT-0.45ST film capacitor at room temperature.

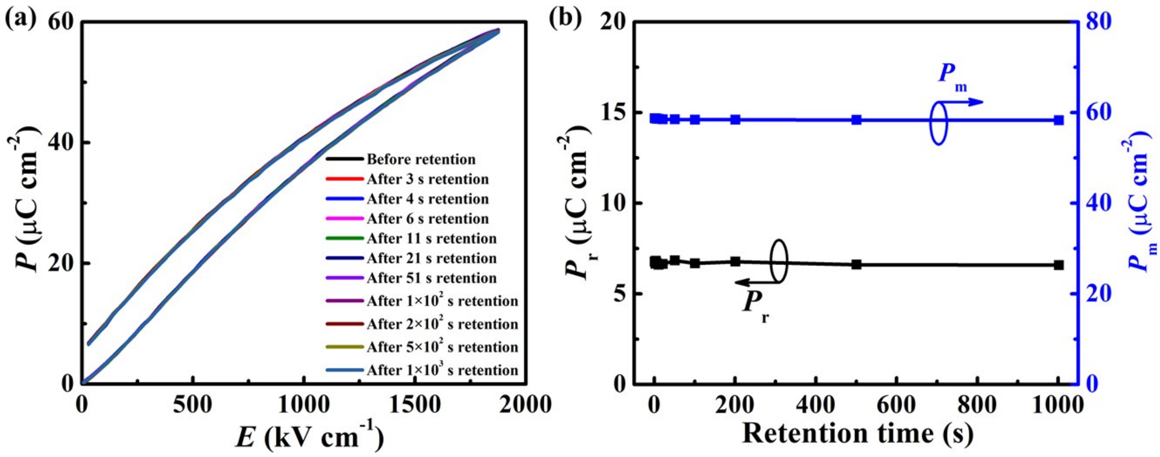

Figure S9. a) The room-temperature unipolar *P*-*E* loops, and b) corresponding P_r and P_m as functions of time during the 10^3 s retention for the Mn:NBT-BT-0.45ST film capacitor.

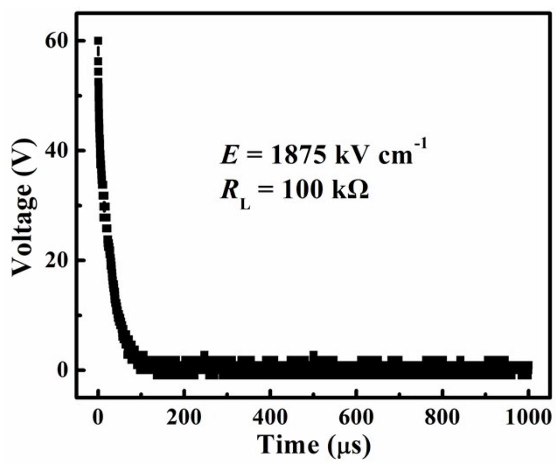

Figure S10. The discharged voltage to a loading resistor (R_L) as a function of time of the Mn:NBT-BT-0.45ST film capacitor, which was measured by a specially designed resistance-capacitance (*RC*) circuit with R_L of 100 kΩ.

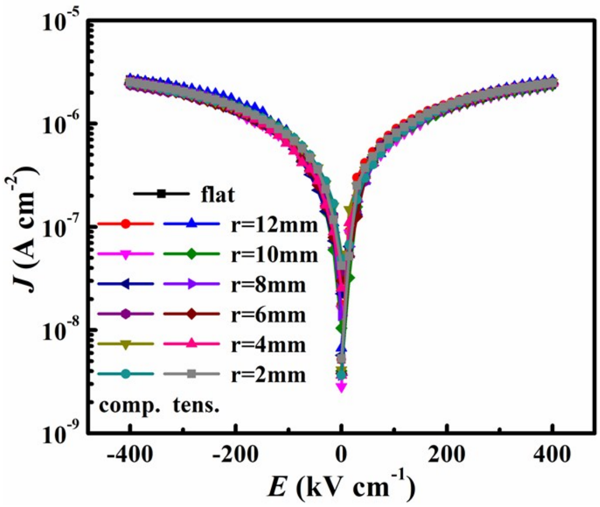

Figure S11. The leakage current density-electric field plots of the flexible Mn:NBT-BT-0.45ST film capacitor measured with various compressive and tensile bending radii.

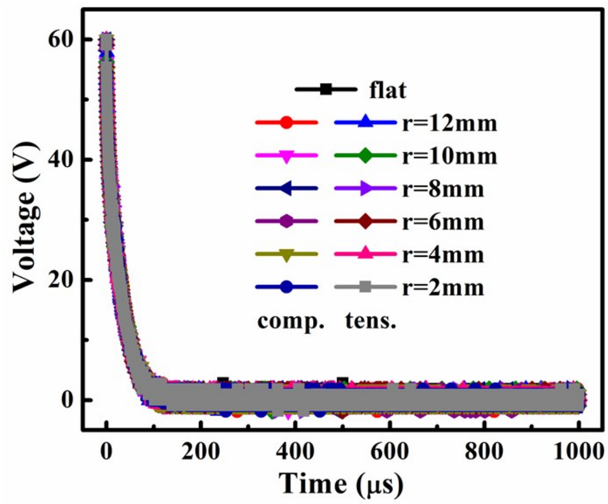

Figure S12. The time-dependent discharged voltage at various radius of curvatures of the flexible Mn:NBT-BT-0.45ST film capacitor at 1875 kV cm^{-1} and room temperature.

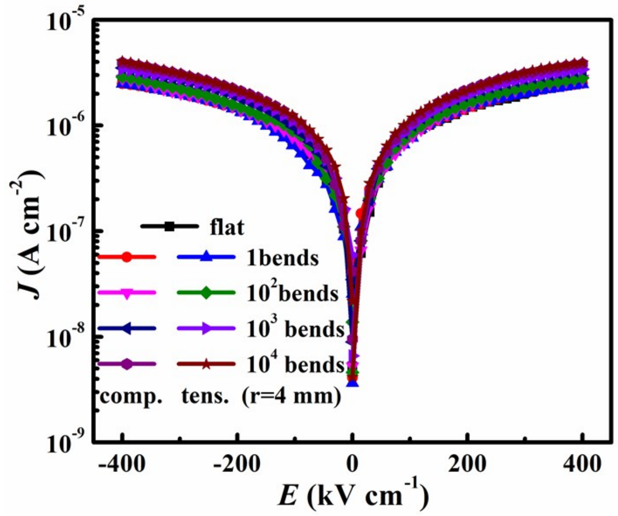

Figure S13. The leakage current density-electric field plots of the flexible Mn:NBT-BT-0.45ST film capacitor measured in its original flat state, and reflattened after various compressive/tensile bending cycles at 4 mm radius.

Table S1. Comparisons of the energy storage property for the Mn:NBT-BT-0.45ST film capacitor and some reported representative organic capacitors.

materials	E (kV/cm)	P_{max}-P_r (μC/cm^2)	W_{rec} (J/cm^3)	η (%)	T (°C)	Bending test	Ref
VDF/PVDF	8200	~14.2	27.3	67	<85	-	[1,2]
P(VDF-TrFE-CTFE)	4000	~10	9	-	<150	-	[3,4]
P(VDF-TrFE-CTFE)/ P(VDF-HFP)	6000		21.9	~65			[5]
BT@BN/PVDF	6000	~6	17.6	~53			[6]
Mn:NBT-BT-0.45ST	2813	69.3	76.1	80.0	-100~200	r=2mm or 10^4 at r=4mm	This work

[1] Z. B. Shen, X. H. Wang, B. C. Luo, L. T. Li, *J. Mater. Chem. A*, 2015, **3**, 18146-18153.

[2] S. M. Yang, T. H. Kim, J. Yoon, T. W. Noh, *Adv. Funct. Mater.*, 2012, **22**, 2310-2317.

[3] B. J. Chu, X. Zhou, K. L. Ren, B. Neese, M. R. Lin, Q. Wang, F. Bauer, Q. M. Zhang, *Science*, 2006, **313**, 334.

[4] W. L. Warren, K. Vanheusden, D. Dimos, G. E. Pike, B. A. Tuttle, *J. Am. Ceram. Soc.*, 1996, **79**, 536-538.

[5] X. T. Ren, N. Meng, H. X. Yan, E. Bilotti, M. J. Reece, *Polymer*, 2019, **168**, 246-254.

[6] S. B. Luo, J. Y. Yu, S. H. Yu, R. Sun, L. Q. Cao, W.-H. Liao, C.-P. Wong, *Adv. Energy Mater.*, 2019, **9**, 1803204.